

Published in final edited form as:

*Biosens Bioelectron.* 2014 February 15; 52: . doi:10.1016/j.bios.2013.08.054.

## Glutamate oxidase biosensor based on mixed ceria and titania nanoparticles for the detection of glutamate in hypoxic environments

Rifat Emrah Özel<sup>#1</sup>, Cristina Ispas<sup>#1</sup>, Mallikarjunarao Ganesana<sup>2</sup>, J.C. Leiter<sup>2</sup>, and Silvana Andreescu<sup>1,\*</sup>

<sup>1</sup>Department of Chemistry and Biomolecular Science, Potsdam, NY 13699-5810, USA

<sup>2</sup>Department of Physiology, Dartmouth Medical School, Lebanon, NH 03756

# These authors contributed equally to this work.

### Abstract

We report on the design and development of a glutamate oxidase (GmOx) microelectrode for measuring L-glutamic acid (GluA) in oxygen-depleted conditions, which is based on the oxygen storage and release capacity of cerium oxides. To fabricate the biosensor, a nanocomposite of oxygen-rich ceria and titania nanoparticles dispersed within a semi-permeable chitosan membrane was co-immobilized with the enzyme GmOx on the surface of a Pt microelectrode. The oxygen delivery capacity of the ceria nanoparticles embedded in a biocompatible chitosan matrix facilitated enzyme stabilization and operation in oxygen free conditions. GluA was measured by amperometry at a working potential of 0.6 V vs Ag/AgCl. Detection limits of 0.594  $\mu\text{M}$  and 0.493  $\mu\text{M}$  and a sensitivity of 793 pA/ $\mu\text{M}$  (RSD 3.49%,  $n=5$ ) and 395 pA/ $\mu\text{M}$  (RSD 2.48%,  $n=5$ ) were recorded in oxygenated and deoxygenated conditions, with response times of 2s and 5s, respectively. The biosensor had good operational stability and selectivity against common interfering substances. Operation of the biosensor was tested in cerebrospinal fluid. Preliminary *in vivo* recording in Sprague-Dawley rats to monitor GluA in the cortex during cerebral ischemia and reperfusion demonstrate a potential application of the biosensor in hypoxic conditions. This method provides a solution to ensure functionality of oxidoreductase enzymes in oxygen-free environments.

### Keywords

microbiosensor; nanoparticles; oxygen; ceria; hypoxia; neurotransmitters; glutamate

### 1. Introduction

*L*-glutamic acid (GluA) or glutamate is one of the most important excitatory signalling molecules in the central nervous system and plays a critical role in a variety of brain functions, *e.g.* memory and learning (Holmes et al. 1993). During hypoxic injury, the normal functioning of the regulatory GluA receptors is compromised, the level of oxygen in the

© 2013 Elsevier B.V. All rights reserved.

\*Corresponding author eandrees@clarkson.edu.

**Publisher's Disclaimer:** This is a PDF file of an unedited manuscript that has been accepted for publication. As a service to our customers we are providing this early version of the manuscript. The manuscript will undergo copyediting, typesetting, and review of the resulting proof before it is published in its final citable form. Please note that during the production process errors may be discovered which could affect the content, and all legal disclaimers that apply to the journal pertain.

tissue decreases (Krajnc et al. 1996), and as a result, the level of extracellular GluA increases (Zemke et al. 2004). Imbalance in oxygen delivery to cells and tissues has been associated with neurodegenerative diseases such as ischemia, epilepsy, Parkinson's and Alzheimer's diseases (Ogunshola and Antoniou 2009). Therefore, development of methods that permit evaluation of GluA levels during hypoxic insults is critical for studying the contribution of excitotoxicity to these disorders.

Analytical techniques commonly used to measure GluA include microdialysis (Baker et al. 2002), capillary electrophoresis (Vyas et al. 2011), fluorescent (Namiki et al. 2007) and luminescent probes (Kiba et al. 2002) and electrochemistry (Walker et al. 2007). Of these, electrochemical methods with microelectrodes allow direct real-time assessment of physiological GluA levels in both *in vitro* and *in vivo* systems with high spatial resolution (Lee et al. 2007). Several types of GluA biosensors have been developed (O'Neill et al. 2004) and some are commercially available (Pinnacle Technology, Inc.). The majority of GluA sensors designed for *in vivo* use are first generation biosensors that utilize glutamate oxidase (GmOx) to enzymatically convert GluA to electrochemically detectable hydrogen peroxide ( $H_2O_2$ ). In this configuration, molecular oxygen is necessary for the formation of  $H_2O_2$ . Therefore, accurate measurements in low-oxygen conditions is a major challenge (McMahon et al. 2007).

Previous investigators have tried to reduce oxygen-dependent variability of oxidoreductase enzymes by including an oxygen chamber as an integral part of the biosensor so that oxygen levels in the region of the enzyme can be maintained at levels sufficient for an adequate sensor response (Simpson; et al. 2006). This approach complicates miniaturization and fabrication of implantable devices. Alternatively, a mixture of graphite powder and perfluorocarbons with high oxygen solubility has been used (Wang et al. 2002; Zhao et al. 2003), but this sensor design has not been miniaturized, and there may be increased toxicity associated with these additional constituents. Few studies address oxygen variability of GmOx biosensors (McMahon et al. 2007). To our knowledge, there is no report of a GmOx biosensor operating in an oxygen-free environment. In this paper, we propose a new technology in which a biocompatible composite of ceria and titania nanoparticles in proximity to the GmOx enzyme dispersed in chitosan is used to provide oxygen to sustain the enzymatic reaction in conditions of oxygen depletion. The method makes use of the oxygen storage and release capacity of biocompatible ceria nanoparticles, which is enhanced in the presence of titania (Njagi et al. 2008).

Cerium oxide nanoparticles have unique redox, auto-catalytic properties (Das et al. 2007). Moreover, ceria is an excellent co-immobilization material for a variety of enzymes such as cholesterol oxidase, glucose oxidase and horseradish peroxidase (Ansari et al. 2009). Its catalytic activity can be exploited to develop highly sensitive, enzymeless  $H_2O_2$  sensors and for the fabrication of third generation biosensors (Ispas et al. 2008). Ceria has high oxygen mobility at its surface (Preda et al. 2011; Zhang et al. 2006b) and a large oxygen diffusion coefficient, which facilitates the conversion between valance states  $Ce^{4+}/Ce^{3+}$  (Dutta et al. 2006) that allow oxygen to be released or stored in its crystalline structure (Wang et al. 2011; Xu et al. 2010). The catalytic and oxygen storage and release capacity are used in this work to fabricate an 'oxygen rich' electrochemical biosensor for the detection of GluA in hypoxic conditions. We show that ceria nanoparticles, in conjunction with titania, embedded in the immobilization environment of GmOx can minimize problems associated with low oxygen levels and maintain the proper functioning of the enzyme, which requires oxygen as co-substrate, enabling this biosensor to work in a hypoxic environment. First, we have performed cyclic voltammetric (CV) characterization of the enzymatic sensor in the presence and absence of oxygen with and without metal oxides in the bioimmobilization matrix and established the optimum operational conditions. Next, the metal oxide GluA

biosensor was studied using amperometry under aerobic and anaerobic conditions in a physiological buffer and further tested in cerebrospinal fluid. This strategy can be used as a general approach for the creation of other oxidoreductase-based biosensors that have requirements for operational functionality in anaerobic conditions.

## 2. Experimental

### 2.1. Reagents

Glutamate oxidase (GmOx) (EC 1.4.3.11, 25 U/vial; from *E. Coli*) was purchased from Yamasa Corporation. Chitosan (practical grade) from shrimp shells, *L*-glutamic acid (99%), titania (nanopowder, 99.5% rutile, cat#637262), ceria (cat#544541), dopamine hydrochloride (DA), 3,4-dihydroxy-*L*-phenylalanine (*L*-DOPA), albumin (BSA) (from bovine serum) and potassium phosphate (monobasic) were obtained from Sigma Aldrich. Sulphuric acid was purchased from Fisher Scientific. *L*-ascorbic acid (AA) (99%), *o*-phenylenediamine (*o*-PD) (98%), serotonin hydrochloride (5HT) and sodium phosphate dibasic (anhydrous) were purchased from Acros Organics. Ascorbate oxidase (AsOx) (EC 1.10.3.3, 1 KU/vial; from *Cucurbita sp.*) was obtained from Alfa Aesar. Silver conductive epoxy was purchased from MG Chemicals, and non-conductive epoxy resin was obtained from Devcon. All solutions were prepared with distilled water collected from Millipore Direct-Q with a resistivity of 18.2  $\Omega\text{-cm}$ .

### 2.2. Instrumentation

Amperometry and CV experiments were conducted using a CHI1030A electrochemical analyzer (CHInstruments Inc.). All electrochemical analyses were performed with a conventional cell with enzyme/nanoparticles/chitosan/*o*-PD/BSA modified platinum wire as working electrode, a Ag/AgCl/3M NaCl (BAS MF-2052, RE-5B) as reference electrode and a platinum wire as a counter electrode. All potentials were referred to the Ag/AgCl reference electrode.

### 2.3. Biosensor fabrication

Platinum working electrodes with a diameter of 125  $\mu\text{m}$  were fabricated from Pt-wires from A-M Systems. The Pt-wire was cut at 2cm length, and the Teflon coating was removed. The biosensing active side was 2 mm in length and bent to a 'v' shape for increased loading of the active material. The inactive portion of the wire was  $\sim$ 5mm in length and was glued to a copper wire with a conductive epoxy. The microelectrode was placed in a pulled glass capillary. The upper end of the capillary was sealed with non-conductive epoxy and cured for 10 min at 100  $^{\circ}\text{C}$ . The electrodes were treated electrochemically next in 0.5 M  $\text{H}_2\text{SO}_4$  through CV in the potential range from  $-0.25$  to 1.65 V at a scan rate of 0.1 V/s for 20 cycles. After the electrochemical treatment, the wire was rinsed thoroughly with distilled water. The clean electrode was electro-coated with *o*-PD by applying a potential of 0.9 V in a stirred solution consisting of 300 mM *o*-PD and 5 mg/ml BSA for 30 min. This method produces a thin, perm-selective and self-sealing film on the electrode surface (Killoran and O'Neill 2008). The electrodes were rinsed with distilled water and immediately modified with the bioactive layer of nanoparticles and enzyme. This modification was made with a mixture containing of 1% chitosan solution,  $\text{CeO}_2/\text{TiO}_2$  dispersion (1:1 ratio of 1 mg/ml of each nanoparticle) and enzyme solution with a ratio of 2:1:1, respectively. The effect of  $\text{CeO}_2/\text{TiO}_2$  loading on sensor response is shown in Figure S1 (supporting information). The enzyme stock solution was 0.1 U/ $\mu\text{l}$  GmOx in 0.1 M PBS (pH=7.4). Two aliquots of 2  $\mu\text{l}$  of this mixture were casted onto *o*-PD modified platinum wire. In the final step, 1  $\mu\text{l}$  of 200 U/ml AsOx stock solution was placed on microelectrode and dried. After each modification step, the electrode was dried under a  $\text{N}_2$  environment. For the control electrodes, GmOx was replaced with the same amount of chitosan. Electrodes were denoted as GmOx/Chit/*o*-PD/Pt

and CeO<sub>2</sub>/TiO<sub>2</sub>/GmOx/Chit/ $\alpha$ -PD/Pt. All electrodes had AsOx incorporated, but it was omitted in the notations. SEM images of sensors can be found in Figure S2.

## 2.4. Electrochemical measurements

Cyclic voltammetry was utilized to characterize the microelectrodes and establish the role of the metal oxides and the effect of oxygen deprivation. CVs were run in potential ranges from -0.25 to 1.65 V and from 0.2 to 1.2 V at a scan rate of 0.1 V/s in 0.1 M PBS (pH=7.4) (Figure S3). Amperometry at a constant applied potential of 0.6 V was used to characterize the biosensor and determine the analytical performance characteristics for the detection of GluA in buffer and CSF. Buffer solutions were deoxygenated by purging nitrogen for 45 min to create anaerobic conditions. The nitrogen flow was maintained throughout the measurements. In control experiments, sensors were tested in the absence of metal oxides under anaerobic conditions. The effect of interferences was determined by co-injecting 5  $\mu$ M GluA and 200  $\mu$ M AA, 2  $\mu$ M DA, 20  $\mu$ M L-DOPA, 10  $\mu$ M 5HT.

## 3. Results and discussion

### 3.1. Biosensor preparation and operation principle

Figure 1 illustrates the design characteristics and the operational principle of the GluA biosensor based on the mixed oxides. To fabricate the biosensor, GmOx was co-immobilized within a chitosan layer containing dispersed ceria-titania nanoparticles and deposited onto a Pt-microelectrode surface. Prior to this modification,  $\alpha$ -PD was electrodeposited onto the working electrode surface to produce a thin, perm-selective and self-sealing film to prevent interferences from highly oxidizable species such as AA (Killoran and O'Neill 2008). The conversion of GluA to  $\alpha$ -ketoglutarate is catalyzed by GmOx and yields electrochemically active H<sub>2</sub>O<sub>2</sub>. The oxygen dependency of this reaction makes the biosensor response sensitive to oxygen variability and prevents functionality in hypoxic conditions. Here, we tested the hypothesis that the surface adsorbed oxygen present on mixed ceria/titania can effectively be used as a co-substrate by GmOx, allowing detection of GluA in oxygen-deficient environments. These materials provide several advantages over previously reported strategies including: (i) biocompatibility, (ii) ability to stabilize enzymes through strong electrostatic interactions and (iii) intrinsic catalytic activity of these materials, thus enhancing stability of the immobilized enzyme and increasing the overall sensitivity of the biosensor. To our knowledge, this is the first report on the use of ceria/titania oxides to provide oxygen to the immobilized GmOx on microelectrode surfaces to enable detection of GluA in low-oxygen conditions.

### 3.2. Voltammetric evaluations of the effect of mixed oxides

To demonstrate the analytical capabilities, the biosensor containing ceria-titania nanoparticles with GmOx was first characterized using CV to examine the oxygen effect and to determine the role of the metal oxides as internal oxygen carriers by evaluating electro-oxidation of GluA in aerobic and anaerobic conditions. Figure 2 shows CVs recorded at the bare and nanoparticle-modified enzyme electrodes in aerobic and anaerobic conditions upon addition of 1 mM GluA in PBS (pH=7.4). The voltammograms demonstrate the oxidation of enzymatically produced H<sub>2</sub>O<sub>2</sub> shown as an increase in the current starting at ~0.3 V and reaching a peak at ~0.6 V. The biosensor containing the ceria-titania nanocomposite showed a small increase in the voltammetric response, which is attributed to the catalytic activity of nanoceria enhancing the oxidation of H<sub>2</sub>O<sub>2</sub> due to the dual oxidation states Ce<sup>3+/4+</sup> (Ornatska et al. 2011). The catalytic efficiency was further enhanced by adding titania (Njagi et al. 2008). In anaerobic conditions in the absence of nanoparticles, the CV did not show any change in the voltammetric current after addition of GluA, compared to the baseline current. This behaviour is due to the absence of oxygen in the microenvironment,

and the inability of the enzyme to convert GluA to H<sub>2</sub>O<sub>2</sub>. On the other hand, under the same experimental conditions, the ceria-titania biosensor showed a clear voltammetric response even in the absence of molecular oxygen in the reaction cell. Moreover, a control biosensor in the presence of ceria-titania, but absence of enzyme, showed no response in the same anaerobic conditions. These findings demonstrate that the nanocomposite mixture facilitates the enzymatic reaction and provides detection capabilities in oxygen-free conditions. Further experiments were conducted to optimize operational conditions to characterize GluA biosensor performance in hypoxic environments.

### 3.3. Optimization of operational parameters: pH and applied potential

The effect of pH was evaluated by measuring the response of the GmOx biosensor after addition of 5  $\mu$ M GluA in a pH range between 5.5 and 8.5 (Figure S5A). The highest current response was obtained at pH 7.4. When measurements were performed at acidic pH, the amperometric current decreased significantly. This is due to decreased enzyme activity, and structural modifications to the chitosan matrix ( $pK_a \sim 6.5$ ), which is known to lose mechanical strength and dissolve at acidic pH (Özel et al. 2011), which leads to enzyme leaching. In contrast in basic conditions, the chitosan film is firm, and the pores within the matrix are narrow, which limits GluA diffusion and access to the immobilized GmOx, slows the response time and reduces the sensitivity of the biosensor. Figure S5B shows the effect of operation potential on the biosensor response in a range from 0.2 to 0.8 V, where the oxidation of H<sub>2</sub>O<sub>2</sub> takes place. The highest current response after additions of 5  $\mu$ M GluA at pH 7.4 was recorded at 0.6 V. Consequently, all further experiments were performed at these operational conditions.

### 3.4. Analytical characteristics in oxygen free and saturated conditions

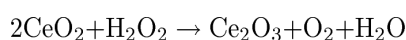
Oxygen sensitivity and the ability of the biosensor to operate in hypoxic conditions were investigated using amperometry at constant potential by measuring the current response following successive additions of 5  $\mu$ M GluA. To assess the role of the metal oxides, a control electrode without the ceria-titania particles was tested. Figure 3 shows comparative amperometric responses of the ceria-titania (CeO<sub>2</sub>/TiO<sub>2</sub>/GmOx/Chit/ $\alpha$ -PD/Pt) and the control (GmOx/Chit/ $\alpha$ -PD/Pt) biosensors in oxygenated and hypoxic conditions.

In the oxygen saturated environment, both the ceria-titania and the control biosensors responded linearly to GluA. Higher responses were observed for the oxide containing biosensor, as predicted by the voltammetric signals in Figure 2A. A linear calibration curve was obtained in the range 5 – 90  $\mu$ M GluA with a sensitivity of 793 pA/ $\mu$ M and a detection limit of 0.594  $\mu$ M for the CeO<sub>2</sub>/TiO<sub>2</sub> GluA biosensor (calculated according to  $3S_b/m$  criteria, where  $S_b$  is the standard deviation of the amperometric signal of PBS and  $m$  is the slope of the calibration curve; Figure 3A, inset). In the same conditions, the sensitivity of GmOx/Chit/ $\alpha$ -PD/Pt was 744 pA/ $\mu$ M. The RSD of the biosensor was 3.49% for  $n=5$  replicate biosensors prepared independently in identical experimental conditions. Taking into consideration the active surface area of the microelectrode ( $\sim 0.79$  mm<sup>2</sup>), the sensitivity of the biosensor described here is better than that reported previously with other glutamate biosensors based on GmOx (Jamal et al. 2010; Zhang et al. 2006a). Table S1 shows a comparative analysis of the analytical performance of this sensor with other GmOx biosensors reported in literature. The short response time,  $\sim 2$ s, indicates a good diffusion rate of the substrate through the chitosan matrix to the active immobilized materials and the electrode surface.

When experiments were performed in the hypoxic environment, the GmOx/Chit/ $\alpha$ -PD/Pt biosensor did not show quantifiable responses to successive additions of GluA (Figure 3B). In this case, a negligible current was observed after the first injection, which could be due to

residual surface adsorbed oxygen in the chitosan matrix. In the same hypoxic conditions, the CeO<sub>2</sub>/TiO<sub>2</sub>/GmOx/Chit/*o*-PD/Pt biosensor displayed well-defined current responses with a linear range from 5 to 50 μM GluA. The sensitivity of the biosensor was 395 pA/μM with a detection limit of 0.493 μM and a RSD of 2.48% for n=5 experiments in the absence of oxygen (Figure 3B, inset). The response time of the sensor increased to ~5s. These results demonstrate the capabilities of this biosensor to operate in oxygen depleted conditions and validate the role of the metal oxides to ensure such function of GmOx. The analytical performance of this biosensor in hypoxic conditions would be suitable to measure physiological changes of glutamate.

The operation of this first generation biosensor in the absolute absence of oxygen is due to a catalytic recycling process of nanoceria and the enzymatically generated H<sub>2</sub>O<sub>2</sub>, and the interchangeable valence states and oxygen vacancies on the surface of exposed nanoparticles (Nolan et al. 2006). These valence states allow oxygen to be stored and released from its structure. While nanoceria can facilitate such processes by itself, the catalytic performance is enhanced in binary nanoparticle mixtures when ceria is in contact with titania. To explain the biosensor functionality in the hypoxic environment, we hypothesize that the surface adsorbed oxygen first participates in the enzymatic reaction catalyzed by GmOx, generating H<sub>2</sub>O<sub>2</sub>. The surface formed H<sub>2</sub>O<sub>2</sub> then reacts with ceria, changing the oxidation state and generating oxygen in the process, thus providing oxygen to sustain the enzymatic reaction as follows:



The ability of ceria nanoparticles to sustain the GmOx reaction depends on the surface area, as well as the amount of the enzymatically generated H<sub>2</sub>O<sub>2</sub> (and thus the amount of GluA that triggers this reaction). Due to this two-step reaction, the response time increases and sensitivity decreases compared to normoxic condition. We have observed that for injections of up to 40 μM GluA, the oxygen stored within the oxide matrix maintains the enzymatic reaction under these conditions, and the biosensor response remains unchanged.

### 3.5. Biosensor selectivity and stability study

Proper functionality of the GmOx biosensor for the analytical quantification of GluA in biological environments relies on the ability of the sensor to selectively detect GluA and be non-responsive to physiological levels of electrochemically active, interfering species that can be oxidized along with H<sub>2</sub>O<sub>2</sub>. The biosensor design incorporates a perm-selective *o*-PD membrane that has been shown previously to prevent access of electro-active species to the electrode surface (O'Neill et al. 2008). In addition to the *o*-PD sieving properties, chitosan rejects AA interferences for CFMEs (Özel et al. 2011). Moreover, the sensor is coated with a chitosan layer containing AsOx to further eliminate AA interferences. The effect of these electrode modifications is discussed in the supporting information, Figure 4S. To assess the effectiveness of these membranes and evaluate biosensor selectivity, the response of the biosensor was investigated against oxidizable molecules that are commonly present in physiological media. The compounds and concentrations tested include 10 μM 5HT, 2 μM DA, 20 μM L-DOPA, 200 μM AA. The amperometric responses of the CeO<sub>2</sub>/TiO<sub>2</sub>/GmOx/Chit/*o*-PD/Pt biosensor at 0.6 V were recorded for each interfering compound and compared to the current response to 5 μM GluA (**Table 1**). The biosensor exhibited high selectivity for GluA versus DA, 5HT, AA and L-DOPA.

The long-term storage stability of the biosensor was evaluated in four different storage conditions: in PBS at pH 7.4; in distilled water and in dry-state at 4°C; and dry-state at -20°C. The response to 5 μM GluA was determined at different time intervals and the

residual activity was calculated relative to the initial signal. The sensor stored in dry-state at 4°C exhibited the highest stability, retaining 80% of the initial activity after 10 days and 55% after 20 days (Figure 4A). The sensors stored in dry-state at -20°C and in PBS and distilled water at 4°C showed 38, 57 and 41%, respectively, residual activity after five day of storage (Figure S6).

The operational stability of the biosensor in the two conditions is shown in Figure 4B. In the aerobic environment, the biosensor showed high operational stability, and no significant change in the response for up to 30 consecutive assays. 75% of the signal was retained after 70 assays. This prolonged stability can be ascribed to the biocompatibility of the chitosan matrix and of the metal oxides, both of which are known to stabilize enzymes through surface entrapment and electrostatic interactions (Krajewska 2004). Under anaerobic conditions, the biosensor recorded a stable response for the first 8 consecutive assays, with a deviation less than 5%. Then the response decreased gradually, probably due to the consumption of surface oxygen of the metal oxide nanoparticles.

### 3.6. Application of the biosensor in cerebrospinal fluid (CSF)

To demonstrate the potential use of this technology in biological fluids, the functionality of the biosensor was further demonstrated in artificial CSF under hypoxic conditions. Figure 5 shows the amperometric response of the biosensor to consecutive additions of 5  $\mu\text{M}$  GluA. The biosensor responded linearly to GluA over a concentration range between 5 and 35  $\mu\text{M}$  with a sensitivity of 156 pA/ $\mu\text{M}$ . While the biosensor sensitivity was lower than that recorded in PBS, which we attribute to the complexity and the electrical resistance of CSF, the current responses in the hypoxic CSF were well defined, and the sensor accurately detected physiological levels of GluA with high reproducibility. The results of these experiments confirm that the biosensor developed herein could be applied for analyses of GluA in biological samples. Preliminary *in vivo* measurements were carried out using rats (experimental details are at SI). Figure S7 demonstrates GluA changes during ischemia/hypoxia and reperfusion periods *in vivo*. Consequently, this biosensor is a good candidate for *in vivo* monitoring of GluA in hypoxic tissue and can potentially used to investigate mechanisms of neurotransmission (abnormalities of which have been associated with several diseases such as cerebral ischemia and Alzheimer's and Parkinson's diseases).

## 4. Conclusions

This work demonstrated that a mixed composite of ceria-titania nanoparticles successfully enables functionality of a first generation GmOx biosensor in hypoxic conditions. The oxygen storage and release capacity of the ceria, associated with the biocompatibility of the chitosan matrix facilitate enzyme stabilization and operation in oxygen free conditions. The biosensor exhibited high reproducibility (RSD 2.48%), good sensitivity (395 pA/ $\mu\text{M}$ ), short response time ( $\sim 5\text{s}$ ) and good linearity over a physiologically useful concentration range under normoxic and hypoxic conditions. It is also demonstrated good functionality in artificial CSF. The microsensor design successfully excluded major interfering species present in physiological media. Since GluA is a mediator of neuronal injury and repair associated with neuronal signalling and brain function during hypoxia, this technology is a promising tool for studying the neurobiology of this neurotransmitter. Preliminary *in vivo* recording in Sprague-Dawley rats demonstrates the potential of this method for real time monitoring of GluA release during cerebral ischemia and reperfusion.

## Supplementary Material

Refer to Web version on PubMed Central for supplementary material.

## Acknowledgments

This work was supported by NIH #R21NS078738-01 to SA and JCL, and by NSF # 0954919 to SA. Any opinions, findings, and conclusions or recommendations expressed in this material are those of the author(s) and do not necessarily reflect the views of the funding agencies.

## References

- Ansari AA, Solanki PR, Malhotra BD. Hydrogen peroxide sensor based on horseradish peroxidase immobilized nanostructured cerium oxide film. *Journal of Biotechnology*. 2009; 142(2):179–184. [PubMed: 19393698]
- Baker DA, Xi Z-X, Shen H, Swanson CJ, Kalivas PW. The Origin and Neuronal Function of In Vivo Nonsynaptic Glutamate. *The Journal of Neuroscience*. 2002; 22(20):9134–9141. [PubMed: 12388621]
- Das M, Patil S, Bhargava N, Kang JF, Riedel LM, Seal S, Hickman JJ. Auto-catalytic ceria nanoparticles offer neuroprotection to adult rat spinal cord neurons. *Biomaterials*. 2007; 28(10):1918–1925. [PubMed: 17222903]
- Dutta P, Pal S, Seehra MS, Shi Y, Eyring EM, Ernst RD. Concentration of Ce<sup>3+</sup> and oxygen vacancies in cerium oxide nanoparticles. *Chemistry of Materials*. 2006; 18(21):5144–5146.
- Holmes GL, Thurber SJ, Liu Z, Stafstrom CE, Gatt A, Mikati MA. Effects of quisqualic acid and glutamate on subsequent learning, emotionality, and seizure susceptibility in the immature and mature animal. *Brain Research*. 1993; 623(2):325–328. [PubMed: 8106123]
- Ispas C, Njagi J, Cates M, Andreescu S. Electrochemical Studies of Ceria as Electrode Material for Sensing and Biosensing Applications. *Journal of The Electrochemical Society*. 2008; 155(8):F169–F176.
- Jamal M, Xu J, Razeeb KM. Disposable biosensor based on immobilisation of glutamate oxidase on Pt nanoparticles modified Au nanowire array electrode. *Biosensors and Bioelectronics*. 2010; 26(4):1420–1424. [PubMed: 20729064]
- Kiba N, Miwa T, Tachibana M, Tani K, Koizumi H. Chemiluminometric Sensor for Simultaneous Determination of l-Glutamate and l-Lysine with Immobilized Oxidases in a Flow Injection System. *Analytical Chemistry*. 2002; 74(6):1269–1274. [PubMed: 11922293]
- Killoran SJ, O'Neill RD. Characterization of permselective coatings electrosynthesized on Pt-Ir from the three phenylenediamine isomers for biosensor applications. *Electrochimica Acta*. 2008; 53(24):7303–7312.
- Krajewska B. Application of chitin- and chitosan-based materials for enzyme immobilizations: a review. *Enzyme and Microbial Technology*. 2004; 35(2–3):126–139.
- Krajnc D, Norton HN, Hadjiconstantinou M. Glutamate, glutamine and glutamine synthetase in the neonatal rat brain following hypoxia. *Brain Research*. 1996; 707(1):134–137. [PubMed: 8866724]
- Lee KH, Kristic K, van Hoff R, Hitti FL, Blaha C, Harris B, Roberts DW, Leiter JC. High-frequency stimulation of the subthalamic nucleus increases glutamate in the subthalamic nucleus of rats as demonstrated by in vivo enzyme-linked glutamate sensor. *Brain Research*. 2007; 1162:121–129. [PubMed: 17618941]
- McMahon CP, Rocchitta G, Kirwan SM, Killoran SJ, Serra PA, Lowry JP, O'Neill RD. Oxygen tolerance of an implantable polymer/enzyme composite glutamate biosensor displaying polycation-enhanced substrate sensitivity. *Biosensors and Bioelectronics*. 2007; 22(7):1466–1473. [PubMed: 16887344]
- Namiki S, Sakamoto H, Iinuma S, Iino M, Hirose K. Optical glutamate sensor for spatiotemporal analysis of synaptic transmission. *European Journal of Neuroscience*. 2007; 25(8):2249–2259. [PubMed: 17445223]
- Njagi J, Ispas C, Andreescu S. Mixed Ceria-Based Metal Oxides Biosensor for Operation in Oxygen Restrictive Environments. *Analytical Chemistry*. 2008; 80(19):7266–7274. [PubMed: 18720950]
- Nolan M, Fearon JE, Watson GW. Oxygen vacancy formation and migration in ceria. *Solid State Ionics*. 2006; 177(35–36):3069–3074.

- O'Neill RD, Lowry JP, Rocchitta G, McMahon CP, Serra PA. Designing sensitive and selective polymer/enzyme composite biosensors for brain monitoring in vivo. *Trac-Trends in Analytical Chemistry*. 2008; 27(1):78–88.
- O'Neill RD, Chang S-C, Lowry JP, McNeil CJ. Comparisons of platinum, gold, palladium and glassy carbon as electrode materials in the design of biosensors for glutamate. *Biosensors and Bioelectronics*. 2004; 19(11):1521–1528. [PubMed: 15093225]
- Ogunshola OO, Antoniou X. Contribution of hypoxia to Alzheimer's disease: is HIF-1 alpha a mediator of neurodegeneration? *Cell Mol Life Sci*. 2009; 66(22):3555–3563. [PubMed: 19763399]
- Ornatska M, Sharpe E, Andreescu D, Andreescu S. Paper Bioassay Based on Ceria Nanoparticles as Colorimetric Probes. *Analytical Chemistry*. 2011; 83(11):4273–4280. [PubMed: 21524141]
- Özel RE, Wallace KN, Andreescu S. Chitosan coated carbon fiber microelectrode for selective in vivo detection of neurotransmitters in live zebrafish embryos. *Analytica Chimica Acta*. 2011; 695(1–2): 89–95. [PubMed: 21601035]
- Preda G, Migani A, Neyman KM, Bromley ST, Illas F, Pacchioni G. Formation of Superoxide Anions on Ceria Nanoparticles by Interaction of Molecular Oxygen with Ce<sup>3+</sup> Sites. *The Journal of Physical Chemistry C*. 2011; 115(13):5817–5822.
- Simpson, P.; Petisce, JR.; Carr-Brendel, V.; Brauker, JH. Electrode systems for electrochemical sensors.. 2006. US Patent 7074307
- Vyas CA, Rawls SM, Raffa RB, Shackman JG. Glutamate and aspartate measurements in individual planaria by rapid capillary electrophoresis. *Journal of Pharmacological and Toxicological Methods*. 2011; 63(1):119–122. [PubMed: 20708699]
- Walker E, Wang J, Hamdi N, Monbouquette HG, Maidment NT. Selective detection of extracellular glutamate in brain tissue using microelectrode arrays coated with over-oxidized polypyrrole. *Analyst*. 2007; 132(11):1107–1111. [PubMed: 17955144]
- Wang D, Kang Y, Doan-Nguyen V, Chen J, Küngas R, Wieder NL, Bakhmutsky K, Gorte RJ, Murray CB. Synthesis and Oxygen Storage Capacity of Two-Dimensional Ceria Nanocrystals. *Angewandte Chemie International Edition*. 2011; 50(19):4378–4381.
- Wang J, Li SF, Mo JW, Porter J, Musameh MM, Dasgupta PK. Oxygen-independent poly(dimethylsiloxane)-based carbon-paste glucose biosensors. *Biosensors and Bioelectronics*. 2002; 17(11-12):999–1003. [PubMed: 12392949]
- Xu JH, Harmer J, Li GQ, Chapman T, Collier P, Longworth S, Tsang SC. Size dependent oxygen buffering capacity of ceria nanocrystals. *Chemical Communications*. 2010; 46(11):1887–1889. [PubMed: 20198242]
- Zemke D, Smith JL, Reeves MJ, Majid A. Ischemia and Ischemic Tolerance in the Brain: an Overview. *NeuroToxicology*. 2004; 25(6):895–904. [PubMed: 15474608]
- Zhang M, Mullens C, Gorski W. Amperometric glutamate biosensor based on chitosan enzyme film. *Electrochimica Acta*. 2006a; 51(21):4528–4532.
- Zhang M, Wang HL, Wang XD, Li WC. Complex impedance study on nano-CeO<sub>2</sub> coating TiO<sub>2</sub>. *Materials and Design*. 2006b; 27(6):489–493.
- Zhao M, Hibbert DB, Gooding JJ. An oxygen-rich fill-and-flow channel biosensor. *Biosensors and Bioelectronics*. 2003; 18(5-6):827–833. [PubMed: 12706598]

### Highlights

- Ceria nanoparticles enable operation of a glutamate oxidase microbiosensor in hypoxic conditions.
- The biosensor is fabricated by co-immobilizing glutamate oxidase with oxygen-rich ceria/titania nanoparticles dispersed in chitosan matrix on a Pt microelectrode.
- The biosensor design is a promising tool for the *in vivo* detection of glutamate in oxygen depleted conditions.

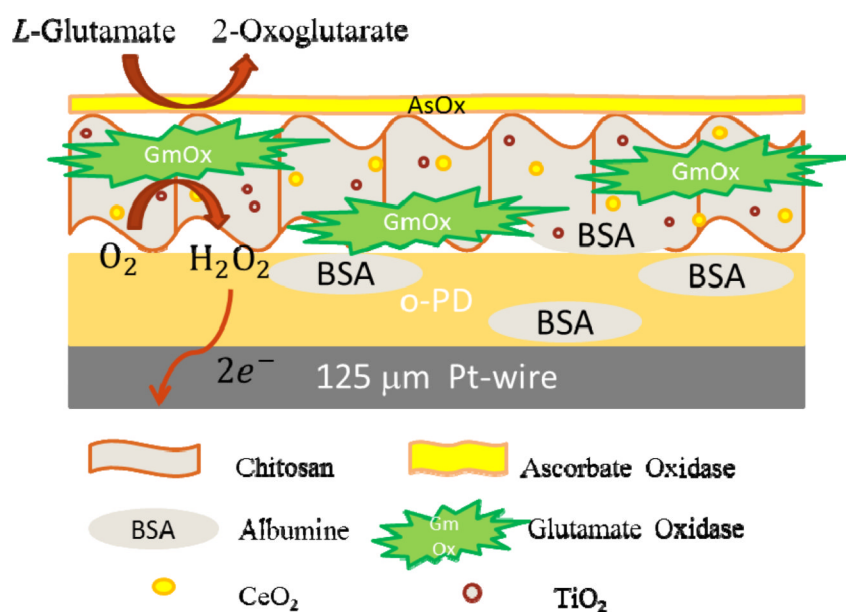


**Figure 1.** Schematic illustration of the biosensor design and the GluA detection principle.

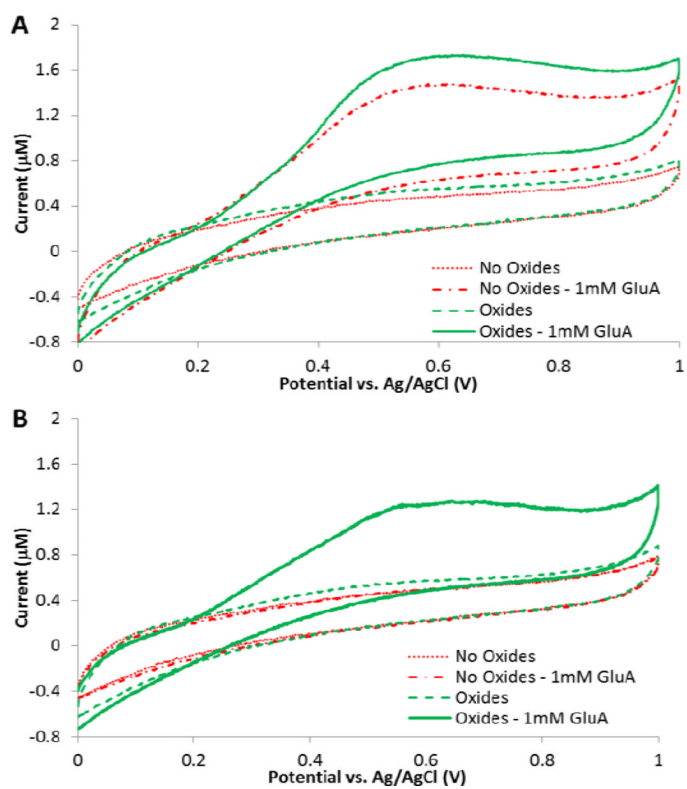


**Figure 2.** Cyclic voltammograms of biosensors with and without ceria-titania oxides in the presence and absence of 1 mM GluA in oxygenated (A) and deoxygenated (B) 0.1 M PBS (pH 7.4). CV scan rate was 0.05 V/s.

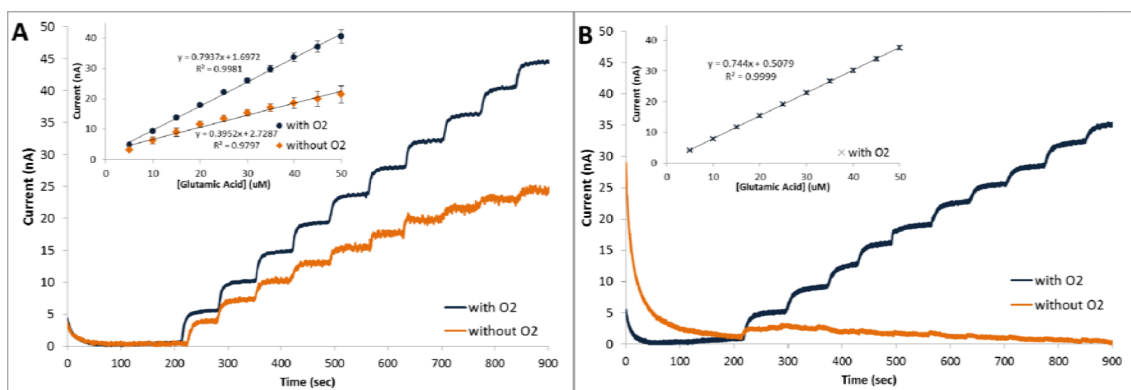


**Figure 3.** Amperometric responses of GmOx biosensors to successive additions of 5  $\mu\text{M}$  GluA in the presence and absence of oxygen with ( $\text{CeO}_2/\text{TiO}_2/\text{GmOx}/\text{Chit}/o\text{-PD}/\text{Pt}$ ) (A), and without ( $\text{GmOx}/\text{Chit}/o\text{-PD}/\text{Pt}$ ) the mixed oxides (B). Insets provide corresponding calibration curves (standard error bars display  $n=5$  replicates).

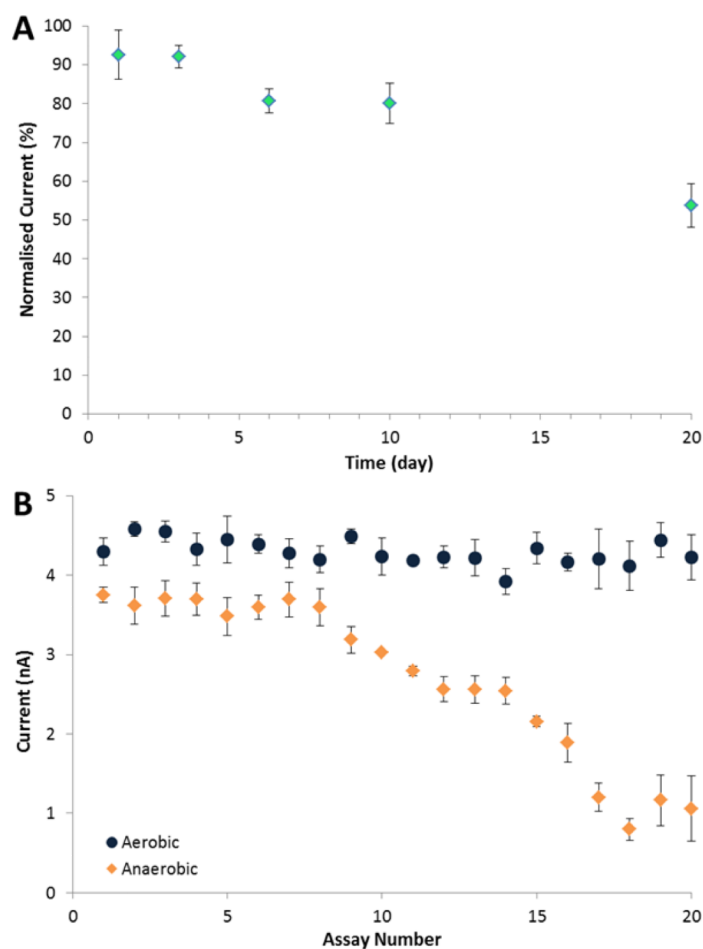


**Figure 4.** Stability measurements of the GluA biosensor. (A) Storage stability at 4°C. (B) Operational stability in aerobic (circles) and anaerobic (diamond) conditions. Current responses recorded for additions of 5  $\mu$ M *L*-glutamic acid at 0.6 V. Standard error bars correspond to  $n=3$  replicates. Supporting electrolyte was 0.1 M PBS (pH 7.4).

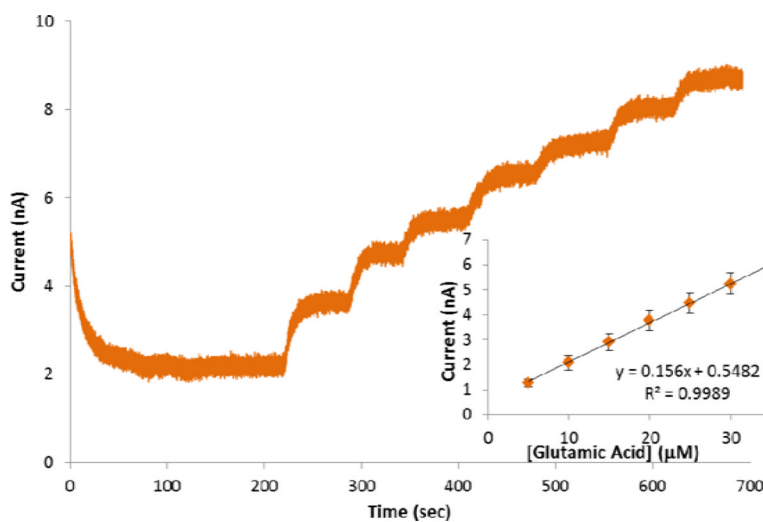


**Figure 5.** Amperometric responses to successive additions of 5  $\mu\text{M}$  GluA and calibration curve (inset) of the GluA biosensor in hypoxic conditions in CSF. Standard error bars correspond to  $n=3$  replicates.

**Table 1**

Effect of interfering compounds on *L*-glutamate microsensor (standard deviations show  $n=3$ ).

Compound	I(pA)/ $\mu$ M
L-GluA	793.7 $\pm$ 27.7
5HT	73.13 $\pm$ 10.5
DA	138 $\pm$ 23.6
L-DOPA	6.15 $\pm$ 0.4
AA	3.60 $\pm$ 1.5